Journal of Power Sources 201 (2012) 179–183

Contents lists available at SciVerse ScienceDirect

Journal of Power Sources

journal homepage: www.elsevier.com/locate/jpowsour

Short communication

Ultrasound-assisted polyol synthesis and electrocatalytic characterization of Pd_xCo alloy and core–shell nanoparticles

Ji-Hoon Jang[a], Chanho Pak[b], Young-Uk Kwon[a,*]

[a] *Department of Chemistry, BK-21 School of Chemical Materials Sciences, SAINT/HINT, Sungkyunkwan University, Suwon 440-746, Republic of Korea*
[b] *Samsung Advanced Institute of Technology, Yongin 446-712, Republic of Korea*

ARTICLE INFO

Article history:
Received 1 August 2011
Received in revised form 17 October 2011
Accepted 26 October 2011
Available online 20 November 2011

Keywords:
Nanomaterials
Ultrasound reaction
Polymer electrolyte membrane fuel cells
Oxygen reduction reaction
Electrocatalysis

ABSTRACT

Carbon supported Co–Pd nanocomposites with two different surface compositions and various Co/Pd ratios have been synthesized by an ultrasound-assisted polyol process. Sonochemical treatment of palladium acetylacetonate and cobalt acetylacetonate in ethylene glycol in the presence of a carbon support without added surfactant, pH adjuster, or stabilizer has produced 4–7 nm Pd_xCo nanoparticles dispersed on the carbon support. The absence of additives has led to purer nanoparticles than produced by conventional wet methods. The structures of nanoparticles – pure Pd, Co–Pd alloy, and core–shell – have been characterized by XRD, TEM, EELS, and STEM. Electrocatalysis of oxygen reduction reactions of the materials have been measured using rotating disk electrodes and are compared with pure Pd/C and commercial Pt/C. The Co–Pd mixed phase samples show higher specific activity than pure Pd/C and comparable performance to commercial Pt/C. The Pd_4Co core–shell structure shows significantly enhanced catalytic activity.

1. Introduction

Bimetallic alloy or core–shell nanoparticles (NPs) that contain transition and noble metals have potential uses in various fields, such as electrocatalysis in fuel cells [1–7] and magnetic materials [8–10]. They are characterized by the structural strain arising from the different sizes of the constituent atoms, which features afford structural diversity and the possibility of tunable properties. In core–shell NPs, the strain at the interface between the core and the shell can be very large, strongly influencing the NPs' properties [1,4,7].

Each of the various techniques reported for the preparation of bimetallic NPs [11–20] has its drawbacks. Multi-step processes for core–shell NPs involve lengthy preparation. Harsh reaction conditions with strong reducing reagents and the presence of surfactants or stabilizing polymers that control NPs' sizes and shapes can cause problems; Liu and Manthiram reported that they reduce catalytic activity [3].

Pd-based NPs, comprising such as Pd_4Co, have been studied with the aim to replace expensive Pt in electrodes [7,15,18]. Suo et al. synthesized Pd_xCo bimetallic NPs with only (1 1 1) surfaces that showed greatly enhanced electrocatalytic activity towards the oxygen reduction reaction (ORR) [7]. Lattice contraction, which reduced the energy of O_2 adsorption onto the catalyst surface, was important in improving ORR activity. The larger strain in core–shell NPs suggests their greater catalytic activity than alloyed NPs. This is supported by some theoretical studies. However, all works characterizing synthesized NPs have studied only one of the two types, with no direct experimental comparison between both of them.

Therefore, this work reports the synthesis and characterization of alloyed and core–shell Pd_4Co NPs on carbon supports (denoted as $Pd_4Co/C(AL)$ and $Pd_4Co/C(CS)$). A novel ultrasound-assisted polyol process was developed for the syntheses. Ultrasound has been used to produce various NPs, including bimetallic NPs [21], however, its use in the synthesis of Pd–Co NPs or core–shell NPs has not been previously reported.

2. Experimental

2.1. Catalysts preparation

Pd_xCo nanoparticles on carbon supports were synthesized by an ultrasound-assisted polyol process with different surface structures – Co-rich cores and Pd-rich shells (CS) and Pd–Co alloys (AL) – and various ratios of Pd/Co (1/0, 1/0.125, 1/0.250, and 1/0.333). The synthetic method was modified to produce each structural type. CS NPs were synthesized by first dispersing cobalt acetylacetonate (Aldrich, $Co(acac)_2$) in ethylene glycol (Samchun Chemical, EG), prepurging it with Ar for 30 min, and irradiating the dispersion with a high-intensity ultrasonic probe (Sonic and

---

* Corresponding author. Tel.: +82 31 290 7070; fax: +82 31 290 7075.
E-mail address: ykwon@skku.edu (Y.-U. Kwon).

0378-7753/$ – see front matter © 2011 Elsevier B.V. All rights reserved.
doi:10.1016/j.jpowsour.2011.10.139

Materials, VC-500, 30% amplitude, 20 kHz, with 13 mm solid probe) for 30 min under Ar to prepare cobalt seeds. Palladium acetylacetonate (Aldrich, $Pd(acac)_2$) and graphitic Ketjen black (GKB, support from SAIT) were subsequently added to the above mixture and irradiated continuously for 150 min. The resulting dark slurry was filtrated through a Nylon membrane (Whatman Int., Ltd.), repeatedly washed with ethanol, and dried under vacuum for 12 h at room temperature. AL NPs were produced similarly, except that $Pd(acac)_2$, $Co(acac)_2$, and GKB were added to the solutions simultaneously. The two sets of materials are denoted as $Pd_xCo/C(CS)$ and $Pd_xCo/C(AL)$, respectively.

2.2. Characterization

Samples were characterized by X-ray diffractometry (XRD, DC/Max 2000, Rigaku, CuKα (λ = 1.54056 Å)) and high-resolution transmission electron microscopy (HR-TEM, JEOL JEM-3011) operating at 300 kV. Elemental compositions were assessed by energy dispersive X-ray spectroscopy (EDS) in conjunction with field emission scanning electron microscopy (FE-SEM, JEOL JSM-7300F). Five different areas of each sample were analyzed to obtain averaged compositions. Individual NPs' elemental compositions were recorded by EDS attached on field emission transmission electron microscopy (FE-TEM, JEOL, JEM-2100F) with a ~1 nm probe under the scanning transmission electron microscope (STEM) mode. Electron energy loss spectroscopy (EELS) analysis was conducted using a ~0.13 nm probe under STEM mode in JEOL ARM200F Cs-corrected TEM.

2.3. Electrochemical analysis

Electrocatalytic behavior was assessed by an Ivium compactstat electrochemical analyzer (Ivium Technology) using a standard three-electrode electrochemical cell and a rotating disk electrode (RDE, Autolab). 3 mg electrocatalyst was dispersed in 1.5 g deionized water by sonication, 5 μL of which was dropped onto a working electrode (glassy carbon, d = 3 mm) and dried in air. 5 μL 0.05 wt% Nafion solution was covered on the working electrode for mechanical protection from the rotation of the RDE. A Pt mesh and a Ag/AgCl electrode were used as the counter and reference electrodes, respectively. The potential range shown in the figures was converted to be referenced to a reversible hydrogen electrode (RHE). To eliminate impurities and to obtain clearer results, the working electrode was repeatedly electrochemically cleaned before each measurement. Cyclic voltammograms (CV) were recorded in aqueous 0.1 M $HClO_4$ at a scan rate of 50 mV s^{-1}. Electrocatalytic surface areas (ESAs) of the electrocatalysts were obtained by calculating the areas of the hydrogen active regions in the CV curves; calibration was made against the 210 μC cm^{-2} of polycrystalline Pt and Pd. Electrocatalytic activity towards the ORR was measured by linear sweep voltammetry (LSV) in 30 min-O_2 saturated electrolyte (0.1 M $HClO_4$) at a scan rate of 5 mV s^{-1} and a rotation speed of 1600 rpm.

3. Results and discussion

3.1. Structural analysis

Syntheses were achieved by the ultrasound irradiation of ethylene glycol solutions of $Pd(acac)_2$ (acac = acetylacetonate) and $Co(acac)_2$ in the presence of carbon supports under Ar. $Pd_4Co/C(CS)$ was synthesized by reacting the Co reagent first to form Co seeds with subsequent addition of the Pd reagent under ultrasound irradiation. $Pd_4Co/C(AL)$ was synthesized with both Co and Pd reagents reacted simultaneously under ultrasound irradiation. The reaction conditions were otherwise the same in both cases. Pd NPs supported on carbon were also similarly prepared without the Co reagent. Ethylene glycol, which may have acted as a mild stabilizing agent, was the only additive used in these syntheses.

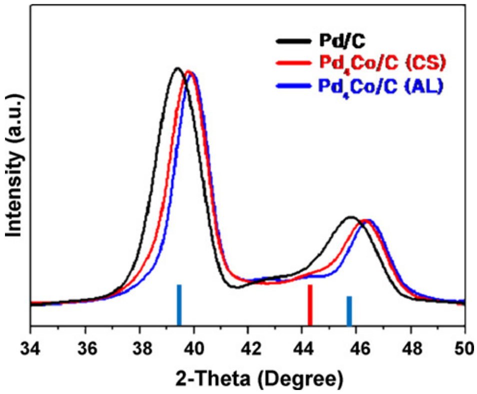

Fig. 1. XRD patterns of Pd/C, $Pd_4Co/C(CS)$, and $Pd_4Co/C(AL)$. Vertical red and blue lines indicate the diffraction peaks of Co (JCPDS, 15-0806) and Pd (JCPDS, 87-0641), respectively, both in face centered cubic structures. (For interpretation of the references to color in this figure legend, the reader is referred to the web version of the article.)

The two samples were shown to have identical compositions, within experimental error, by EDS/SEM carried out (Table S1). Macroscopic homogeneity of the electrocatalysts was confirmed by taking EDS measurement at five different areas (*ca.* 1 × 1 μm^2) of each sample. EDS/TEM was also used to verify the uniform compositions of individual NPs within the samples (Fig. S1).

Fig. 1 shows the XRD patterns of the materials. The Scherrer equation was used to calculate particles sizes: 6.1 nm for Pd/C, 6.3 nm for $Pd_4Co/C(CS)$, and 7.3 nm for $Pd_4Co/C(AL)$. The XRD patterns were indexed as face-centered cubic unit cells with a = 3.96 Å for Pd/C, a = 3.90 Å for $Pd_4Co/C(CS)$, and a = 3.88 Å for $Pd_4Co/C(AL)$. The lattice parameter of Pd/C was slightly larger than that of pure Pd (3.91 Å), indicating hydrogen absorption [22–25]. Pd_4Co showed smaller lattice parameters than Pd due to the incorporation of smaller Co atoms in the Pd lattice. The XRD patterns clearly show that, though small, $Pd_4Co/C(CS)$ has a larger lattice parameter than $Pd_4Co/C(AL)$. Since their compositions are identical, this is likely due to the differences of elemental distribution.

The Pd_4Co NPs were studied by TEM and EELS in conjunction with STEM. The low-magnification TEM image of Pd/C (Fig. S2(a)) shows its 5–8 nm spherical NPs well-dispersed on the carbon support. The magnified TEM image of a Pd NP (Fig. 2(a)) shows its polycrystalline nature with lattice fringes of (1 1 1) and (2 0 0) plains. Both Pd_4Co/C samples (Figs. S2(b) and (c)) comprised 5–8 nm NPs; triangular and spherical shaped NPs are mixed. All the triangular NPs appear to be single crystalline – the triangular faces were (1 1 1) facets (Figs. 2(b) and (d)). The spherical NPs show both single-crystallinity (Figs. 2(c) and (e)) and polycrystallinity (Fig. 2(f)). Therefore, both the Pd_4Co/C samples have larger fractions of (1 1 1) facets than Pd/C. The incorporation of Co appears to lower the surface energy of the NPs, inducing larger crystallites than in pure Pd. This does not necessarily imply different elemental compositions across differently shaped NPs: because the EDS spectra of differently shaped individual NPs showed similar compositions (Fig. S1). Also, the average lattice spacing of differently shaped NPs, taken over at least ten repeating units, are close to each other. We used EELS analysis to see the direct evidence for the core–shell structure of $Pd_4Co/C(CS)$. Although EELS signals are very weak because the energy losses are recorded, it has much higher spatial resolution than that of EDS. The core–shell structure of $Pd_4Co/C(CS)$ was confirmed by EELS measurements of the edges